Pressure and temperature measurements in the annulus between the piston and cylinder of a simple dead-weight piston gauge

B. E. Welch and Vern E. Bean

Center for Absolute Physical Quantities, National Bureau of Standards, Washington, D. C. 20234

(Received 2 March 1984; accepted for publication 20 July 1984)

Precise and accurate pressure measurements are obtained using appropriately designed and operated piston gauges. Elastic distortion of the piston and cylinder is the leading cause of inaccuracy in measurement of higher pressures. The distortion depends upon the ratio of the pressure in the annulus between the piston and the cylinder to the pressure under the piston. Heretofore, as the proper value of this ratio or a method to determine it was unknown, the practice has been to assume a value of 0.5 when calculating distortion effects. In this work, the pressure and temperature of the fluid in the annulus have been measured along the working length of the piston and the cylinder. The model for the pressure ratio proposed by Bass on the basis of the clearance between the piston and cylinder is in excellent agreement with the pressure measurements. The appropriate value of the pressure ratio for the calculation of the distortion is marked by a sharp decrease in the slope of the pressure ratio curve. The corresponding value on the length axis is the appropriate location to calculate the area of the gauge from the dimensional measurements. The temperature measurements indicate that the temperature gradient along the cylinder is due solely to the flow of fluid up through the annulus and, for the most extreme case, was less than 60 mK.

INTRODUCTION

A piston gauge consists of a carefully prepared piston of known diameter fitted into a matching cylinder of known diameter filled with fluid. The piston is loaded with known weights and rotated to relieve friction and to assure concentricity. The pressure P_s in the fluid is defined as the ratio of the downward force due to the weights to the effective area of the piston and cylinder assembly. Other names for such instruments include: pressure balance, dead-weight tester, piston manometer, dead-weight gauge, and free piston gauge. Detailed discussions of this type of apparatus are found in the literature.[1-3]

The change in the effective area due to the elastic distortion of the piston and cylinder as the pressure changes is a leading cause of inaccuracy. The magnitude of the inaccuracy is dependent upon the gauge design, materials from which the piston and cylinder are made, and the pressure. Distortion effects have been reported in piston gauges operating at pressures as low as 160 kPa.[4]

There are four ways to deal with elastic distortion. They are:

(1) *Calculation.* If the temperature is constant so that thermal expansion effects can be ignored, the effective area A_e of the piston gauge can be expressed as

$$A_e = A_0(1 + bP_s), \tag{1}$$

where A_0 is the mean of the piston and cylinder areas at zero pressure, and b is the elastic distortion coefficient.[1]

For piston gauges of certain geometries, b can be calculated from theory. For a right circular cylinder, free of end loading or external pressure, and a solid piston, the elastic distortion coefficient can be written as[1,5]

$$b = \underbrace{\left(\frac{\mu}{E} + \frac{P_a}{P_s}\frac{(\mu - 1)}{E}\right)}_{\text{piston}} + \underbrace{\left(\frac{P_a}{P_s}\frac{(1+\mu)w^2 + (1-\mu)}{E(w^2-1)}\right)}_{\text{cylinder}}, \tag{2}$$

where the first term in brackets is the contribution due to the piston and second is that of the cylinder. In Eq. (2), μ is Poisson's ratio, E is Young's modulus, P_a is the pressure in the annulus between the piston and the cylinder, and w is the ratio of the cylinder's outer diameter to its inner diameter. The troublesome parameter of Eq. (2) is P_a. It is a function of the cylinder working length and ranges in value from zero to P_s. Because the appropriate value of P_a to be used in Eq. (2) or a method to obtain it was unknown, it has been customary to arbitrarily assign $P_a = 0.5P_s$. The determination of the appropriate value of P_a is the purpose of this paper.

(2) *Calibration.* When known pressures are used to calibrate a piston gauge, b can be determined from the calibration data by computer-fitting appropriate models such as Eq. (1). The method applies, in principle, to any piston gauge. The only requirement is that the calibration system and the piston gauge operate at a sufficient level of precision, say on the order of 10 ppm (10^{-5}).

(3) *Controlled clearance.* A controlled clearance piston gauge is equipped with a means to provide an auxiliary pressure to the external wall of the cylinder in order to counteract the distorting effects due to the internal pressure. With the distortion of the cylinder controlled, the elastic distortion need be calculated only for the piston. As the effect of the elastic distortion of the cylinder is typically five to ten times that of the piston, control of the cylinder distortion can offer a significant advantage, particularly at very high pressures.

(4) *Similarity method.* The similarity method[6] assumes that two idealized piston and cylinder systems made of isotropic elastic material, having perfect cylindrical and concentric geometry, and with known elastic moduli, are available and that the change of the radii of the pistons and cylinders due to P_a may be taken to be proportional to P_a at the same position. By experimentally comparing the two gauges in a cross-float arrangement,[1] the ratio of the effective areas can be determined. The distortion coefficients for both gauges can then be calculated using the area data and the values of the moduli.

Each of these four methods of accounting for the elastic distortion offers its own set of advantages and disadvantages. In the view of the present authors, the greatest opportunity for reduction of the inaccuracy in pressure measurements due to elastic distortion lies in a better understanding of the conditions in the fluid in the annular space, which should yield an improved ability to calculate the distortion coefficient. To this end, three series of measurements were carried out:

(a) The pressure profile in the annular space between the piston and cylinder has been measured using miniature pressure transducers placed along the working length of the cylinder. The region where the slope of the pressure profile curve sharply decreases is of special interest because of its implications in calculating elastic distortion.

(b) Multiple-dimensional measurements were carried out over the working length of both the piston and cylinder. From these measurements a radial clearance profile was developed which was used to calculate the pressure profile using the model due to Bass.[4] The calculated and measured pressure profiles are in excellent agreement.

(c) The temperature profile in the fluid between the piston and cylinder has also been measured with the effects due to viscous drag of the fluid, rotation of the piston, and adiabatic heating being separately determined.

I. EXPERIMENTAL APPARATUS

A. Piston and cylinder

The piston and cylinder were originally off-the-shelf, commercial items, the cylinder requiring modification by NBS to accommodate the miniature pressure transducers. The selected model of piston and cylinder assembly offered several advantages: (1) a pressure range (up to 21 MPa) compatible with commercially available pressure transducers; (2) a top loading piston permitting easy access to the transducers; (3) a piston engagement length sufficiently long so that a large number of measurement ports could be drilled; and (4) cylinder walls thick enough to allow for support and seal of the transducers. A schematic diagram of the piston and cylinder is shown in Fig. 1. The cylinder has a nominal bore diameter of 0.4 cm and a piston engagement length L of 2.7 cm. Eight equally spaced flats parallel to the cylinder axis were milled along the outer diameter of the cylinder. Within the engagement length, a series of 35 evenly spaced ports, 0.076 cm in diameter, were drilled along the length of the flats through the wall of the cylinder. Two additional ports

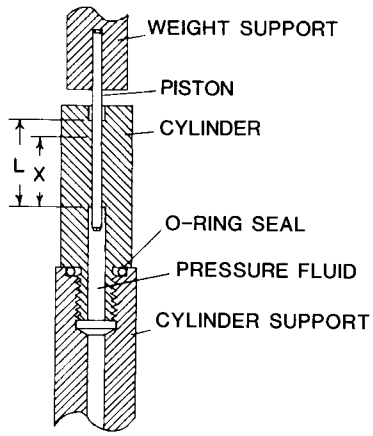

FIG. 1. Schematic sketch of the piston and cylinder assembly.

were drilled above and below the engagement length. The locus of the series of ports was in the shape of a helix, with a vertical separation of 0.079 cm from one port to the next.

Two miniature pressure transducers were used for the pressure measurements. One remained in the bottom-most port to monitor the system and the other was moved from port to port to measure the gradient. Those ports not in use during a particular measurement were sealed using stainless-steel binding head screws with the threads adjacent to the head removed to accommodate an O ring. The assembled piston gauge with the two pressure transducers installed is shown in Fig. 2.

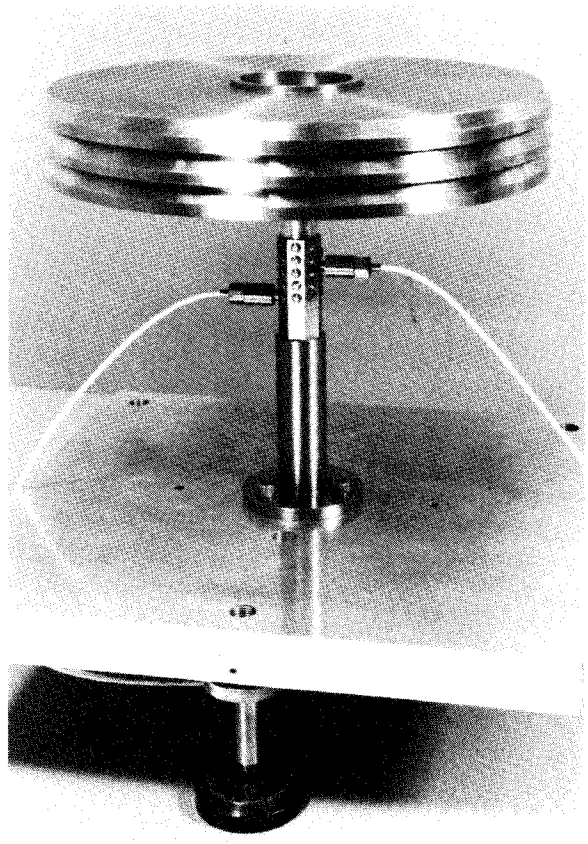

FIG. 2. Photograph of the experimental piston gauge with the pressure transducers installed.

The piston and cylinder were carefully lapped using 0.05-μ alumina polishing compound. The parts were then ultrasonically cleaned and assembled. As a final lapping, the piston and cylinder were operated for several hours using a fine oil with periodic diassembly and recleaning.

B. Pressure transducers

One of the miniature transducers is shown in Fig. 3. The transducers are of the bonded semiconductor strain gauge type. A 5 1/2 digit multiplexed digital voltmeter was used to monitor the output and the regulated dc power supply on the input. Prior to calibration, the transducers were tested for short-term drift, torque effects, zero shift, and the results of exercising over the full pressure range. The transducers were calibrated both before and after the pressure profile measurements, using a piston gauge with increasing and decreasing pressures for a total of 21 observations. The inaccuracy of the gradient measuring transducer was on the order of 0.03%. The change in the calibration of each transducer over the 9-month period between calibrations amounts to a fraction of a percent and is negligible for the present purpose. An adapter with an O-ring seal was used to connect the transducer to the cylinder, as shown in Fig. 3. The adapter was filled with oil before attaching the transducer and the combination remained together during the measurements.

C. Thermocouples

Thermocouples were used to make two differential temperature measurements: (a) between the fluid at the lower end of the piston and ambient and (b) between the fluid in the annulus and ambient. The thermocouples were made of copper and constantan wire, 0.0076 cm in diameter, insulated with varnish. Each thermocouple was anchored with epoxy into a fixture as shown in Fig. 3 such that when the fixture was mounted on the cylinder, the junction was in close proximity to the annular space. The ambient temperature reference junctions of both thermocouples were connected together and anchored to a liquid-in-glass thermometer inserted in a thermally insulated copper block.

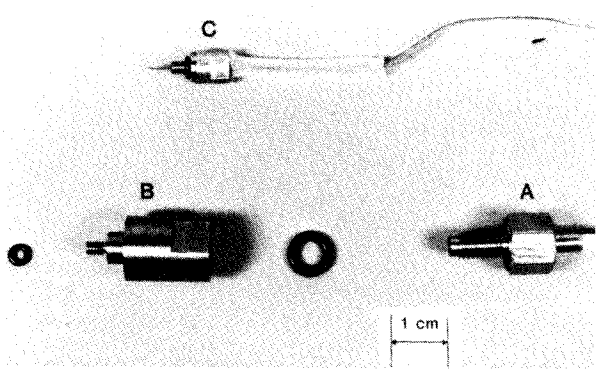

FIG. 3. Pressure transducer (A) with the adapter (B) and a thermocouple probe (C).

II. PERFORMANCE AND DIMENSIONAL MEASUREMENTS

Several preliminary tests were done to characterize the piston gauge before making the pressure and temperature profile measurements in order to examine the performance of the piston gauge in operation.

A. Rotational effects

To determine the optimum rotational conditions, the gauge was operated at four pressures over its range, with two different fluids and various positions of alignment of weights. The two fluids are spindle oils that are commonly used in piston gauges and herein designated as fluid 34 and fluid 38. The viscosity of fluid 34 is 0.141 P, for fluid 38 it is 0.344 P, both at 23°C and atomspheric pressure. The pressure coefficient for both fluids is essentially equal up to 21 MPa. With careful alignment of the weight stack such that the force due to the weights acted only vertically along the axis of the piston, the piston would continue to rotate for a period of 30 to 50 min in a reproducible fashion depending upon load, fluid, and initial rate of rotation. If the weights were stacked so as to allow any horizontal force components, rotation could cease within several minutes. The rate of rotation as a function of time for four different conditions and with the correct weight alignment is plotted in Fig. 4. The two curves where fluid 34 is the pressure fluid are at the same pressure but differ by the initial rate of rotation. The two curves where fluid 38 was used demonstrate the effect of increased viscosity and increased inertial mass on the piston.

The direction of rotation of the piston had a negligible effect on performance.

Within the sensitivity of the pressure transducers, speeds of rotation between 30 and 60 rpm did not appear to have a significant effect on the pressure in the annulus. As the speed of rotation was reduced substantially, the pressure in the annulus would generally increase. For example, with a system pressure of 2.3 MPa and the transducer placed two-

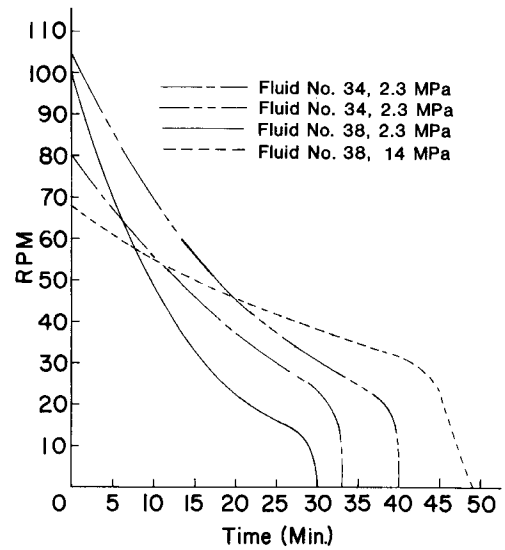

FIG. 4. Piston rotational decay rate. The curves represent the average of the data points. Individual data points are omitted for clarity.

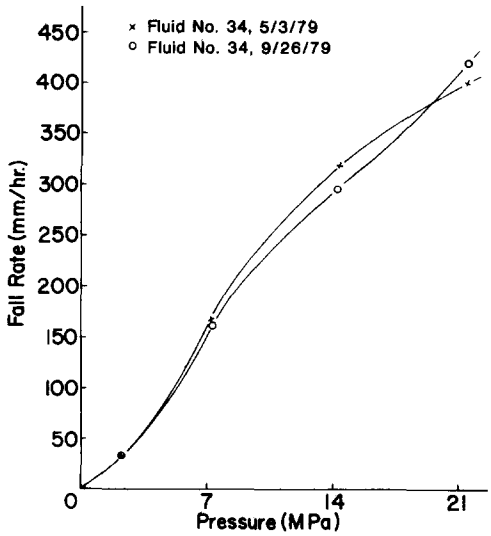

FIG. 5. Piston fall rate. The smooth curve is intended only as a guide to the eye.

thirds of the way down the engagement length of the cylinder, the pressure at that point increased by 2% at the time the speed of rotation went to zero. In all cases the piston and weights were rotated by hand.

Based upon these data it was decided to operate the gauge at 40 rpm.

B. Fall rate

Measurements of the rate at which the piston falls into the cylinder while the gauge is in operation are a useful way of detecting wear. The fall rates measured before and after the pressure profile measurements indicate negligible changes occurred in the piston gauge. The fall rate measurements are shown in Fig. 5.

C. Piston position effects

Any deviation from perfectly cylindrical geometry in either the piston or the cylinder could cause the effective area to be a function of the rotational position of the piston with respect to the cylinder. With a slight out-of-roundness and/or with an eccentric load, the piston would operate as a rotating vane and a pumping action could result. As the pressure measured at a particular point along the engagement length did cycle between two extreme values, the average of these values was used for the pressure profile. For the worst case the variation in pressure from the average value was less than $\pm 0.2\%$.

Vertical displacement of the piston with respect to the cylinder also changed the values of the measured pressure along the annular space due to variation in piston diameter along its length. To maintain the same mean radial clearance between piston and cylinder at a given point, the gauge was always operated at a reference level 0.5 cm above the bottom stop.

D. Intercomparison with standard pressure gauge

The piston gauge was intercompared with a NBS transfer standard piston gauge using a standard calibration procedure.[1] The transfer standard had been previously calibrated using a controlled clearance primary standard piston gauge. Of the eight different calibration equations considered, Eq. (1) best represents the data. The results of the calibration are given in Table I. Observations at ten pressures were obtained over the range. The inaccuracy from random sources was taken as three times the standard deviation of the residuals as determined by statistical analysis of the calibration data. The inaccuracy from systematic sources represents the bound of errors due to the standard.

E. Dimensional measurements

The piston and cylinder were measured for roundness, absolute diameters, and relative tapers under the direction of the NBS Dimensional Metrology Group. Camber was not measured but the excellent performance of the gauge indicated that it could not have been excessive. Dimensional measurements were made at 20°C. Roundness measurements were carried out at 16 locations over the effective length of the piston and cylinder.

Absolute diameter measurements of the piston were made at the center of the engagement length. Two different comparators were used for these measurements. From the two methods an average of $0.405\,016 \pm 0.000\,015$ cm was determined to be the best value for the piston diameter.

An internal comparator was used to measure the absolute bore diameter of the cylinder yielding a mean value of $0.405\,338 \pm 0.000\,015$ cm. Relative diameter measurements were then carried out and referenced to the absolute values for both the piston and the cylinder. From these data the radial clearance profile was constructed as shown in Fig. 6.

TABLE I. Piston gauge intercomparison at 23 °C.

		Uncertainty		
Coefficient	Value	Random	Systematic	Total
A_0	$1.289\,74 \times 10^{-5}$ m^2	16 ppm	61 ppm	77 ppm
b	4.21×10^{-12}/Pa	0.95×10^{-12}/Pa	1.2×10^{-12}/Pa	2.2×10^{-12}/Pa

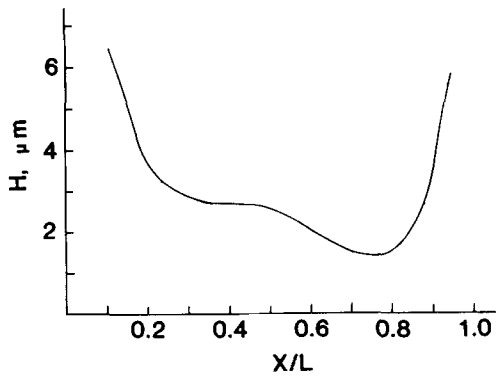

FIG. 6. Radial clearance between piston and cylinder as a function of the ratio of the position along the cylinder to its length as determined from the measured diameters.

III. PRESSURE MEASUREMENTS

A. Profile

Starting with the less viscous of the two oils, fluid 34, the pressure profile was measured over the total cylinder working length for four nominal system pressures. In Fig. 7 the ratio of the annular pressure to the system pressure P_a/P_s, is plotted as a function of the ratio of the location along the cylinder to the total cylinder working length, X/L. The four curves are essentially identical with one minor exception. The curves deviate near the center of the cylinder working length. There appears to be an ordering in the deviation, suggesting that it is a function of pressure. While unequal numbers of measurements for each curve have limited the detailed definition of the curves in this region, the ordering is consistent with the effect one might expect from elastic deformation. As the system pressure increases, the annulus tends to widen with the result that the pressure ratio curves show a shift to higher values of the cylinder working length. In the absence of distortion, the four curves would be expected to be identical.

The model suggested by Bass[4] can be used to calculate the value of P_a/P_s at any position along the cylinder working length, given the dimensional measurements for the piston and cylinder. The Bass equation is obtained by integrating the mass flow equation assuming the viscosity to be independent of pressure, and is given by

$$\frac{P_a(X/L)}{P_s} = 1 - \frac{P_s - P_L}{P_s} \frac{\int_0^{X/L} d(X_1/L)/H^3(X_1/L)}{\int_0^1 d(X_2/L)/H^3(X_2/L)}, \tag{3}$$

where P_L is the pressure at the top end of the cylinder and $H(X/L)$ is the radial clearance between the piston and cylinder. Calculated values of $P_a(X/L)/P_s$ using the values of $H(X/L)$ from Fig. 6 are plotted in Fig. 8 along with the values measured at 2.3 MPa for comparison. The excellent agreement between the calculated and the measured pressure profiles is an indication that the pressure profile will be different for each piston and cylinder combination due to dimensional variances arising from manufacturing tolerances as suggested by Zhokhovskii.[7]

B. Elastic distortion

The task at hand is to select the appropriate value of $P_a(X/L)P_s$ of Fig. 8 to use in Eq. (2) to calculate the distortion coefficient b. Regarding that appropriate value, Johnson and Newhall[5] wrote: "In the piston gauge the pressure varies along the length of the crevice between piston and cylinder. At the bottom it equals the pressure being measured; at the top it falls to zero. The fall of pressure probably will be concentrated in a small portion of the length. The effective pressure in the crevice to be used in calculating the distortion, will depend on the location of the region of falling pressure."

If the pressure profile had been a step function, it is obvious that the region of falling pressure referred to would be at the corner of the step. The corner of the step would also correspond to a break in the slope of the pressure profile curve, which was a clue that the slopes of the curves of Fig. 8 should be examined.

Since the pressure profile curves of Fig. 8 are based on evenly spaced measurements of pressure or piston and cylin-

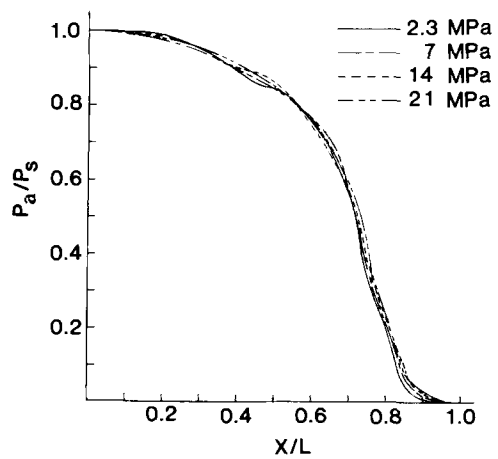

FIG. 7. Ratio of the pressure in the annulus between the piston and cylinder to the pressure in the system measured at four stystem pressures as a function of the ratio of the position along the cylinder to its length for fluid 34. Discrete data points have been omitted for clarity.

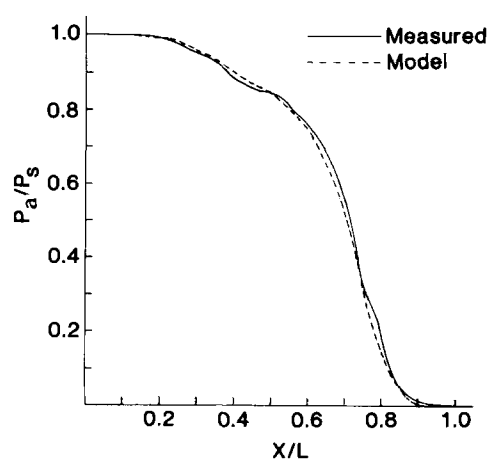

FIG. 8. Ratio of the pressure in the annulus between piston and cylinder to the pressure in the system measured at 2.3 MPa compared with the same ratio calculated from the Bass model using dimensional measurements. Discrete data points have been omitted for clarity.

der dimensions; a good approximation to the slopes can be obtained by taking the differences in $P_a(X/L)P_s$ values between successive pairs of data points and dividing by the engagement length increment for each curve. The slopes thus obtained are plotted in Fig. 9. In each case there is a definite downward break in the slope, the coordinates of which have been determined graphically. For the measured pressure profile curve, it occurs in the neighborhood of $X/L = 0.564$ with a corresponding value of $P_a(0.564)/P_s$ of 0.842. For the curve calculated from the Bass model, the break in the slope occurs in the neighborhood of $X/L = 0.574$ with a corresponding $P_a(0.574)/P_s$ value of 0.828. The values of b calculated from these ratios using Eq. (2) are 4.34×10^{-12} and 4.29×10^{-12} Pa^{-1} for the measured pressure profile and the Bass model, respectively, which differ by only 1.2%. When compared with the value of b obtained from the piston gauge calibration data, that from the measured pressure profile is 3.1% higher; the value from the Bass model is 1.9% higher. The agreement is remarkably good. The values of b are summarized in Table II.

Equation (2) is based on three simplifying assumptions which are not appropriate for a piston gauge. They are: (a) the pressure is uniform over the entire length of the cylinder, (b) the length of the cylinder is infinite, and (c) the elemental segments of the cylinder made by radial planes dx apart along the cylindrical axis suffer no shear stresses in those planes. Consequently, the values of b calculated using Eq. (2) will be too large—a result consistent with the observations and possibly fortuitous.

The radial holes in the cylinder were not considered when computing b using Eq. (2), but do influence the value of b determined from the piston gauge calibration data. The holes will result in a slightly larger value from the calibration data than would be obtained from the same cylinder without the holes. The excellent agreement between the values of b calculated using the break in the slope of the pressure profile curve to determine the pressure ratio and that determined from the calibration data is strong evidence that the break in the slope identifies the location of the effective area along the piston. One may think of it as the region where the pressure "seal" between the piston and the cylinder takes place.

By way of contrast, using the conventional and arbitrary value of $P_a/P_s = 0.5$, the calculated value of b is 3.19×10^{-12} Pa^{-1}, which is 24% below the value obtained from the pressure calibration data. In order to estimate the inaccuracy in b obtained using Eq. (2), the effect of the assumptions applied in the deviation of that equation must be evaluated, a nontrivial task now worth doing but yet to be done.

The similarity method has been applied to a steel piston and cylinder with elastic properties similar to those used in the present measurements. The value of b is 4.06×10^{-12} Pa^{-1}, which is not far removed from the present results, but the differences on cylinder geometry render a detailed comparison meaningless.[6]

C. Area

The area A_0 of the piston–cylinder assembly at atmospheric pressure was calculated along the cylinder working length from the dimensional measurements as the average of the areas of the piston and cylinder corrected to 23°C and is plotted in Fig. 10. The value of A_0 was also determined by a pressure calibration using a NBS standard piston gauge with the result of $1.289\,74\times10^{-5}$ m^2, and is also indicated in Fig. 10. The intersection of these two curves corresponds to an X/L value of 0.585, which is in excellent agreement with the X/L value where the break in the slope occurs in the pressure profile curves of Fig. 8. The values are 0.565 and 0.574 for the measured pressure profile and the Bass model profile, respectively. This agreement is added evidence that the location of the effective area is marked by the break in the slope in the pressure profile curve and not necessarily in the region of minimum clearance between piston and cylinder.

The combined results listed in Table II and those shown in Fig. 10, suggest a possible method for determining the effective area of a simple piston gauge based on dimensional measurements. The method is: (1) Determine the pressure

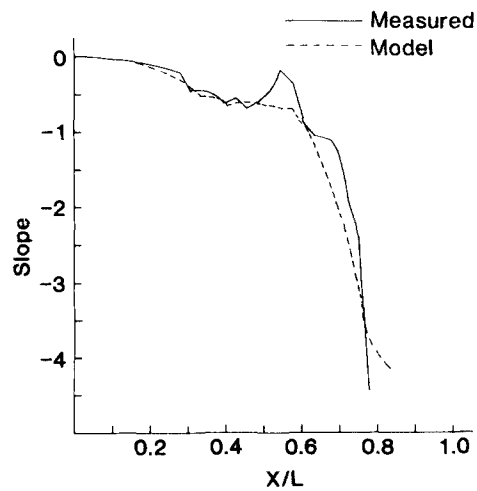

FIG. 9. Slopes of the pressure profile curves obtained using the Bass model measurement at 2.3 MPa and by calculation using the Bass model and dimensional measurements. The downward break in the measured curve occurs at $X/L = 0.565$; for the Bass model it occurs at $X/L = 0.574$.

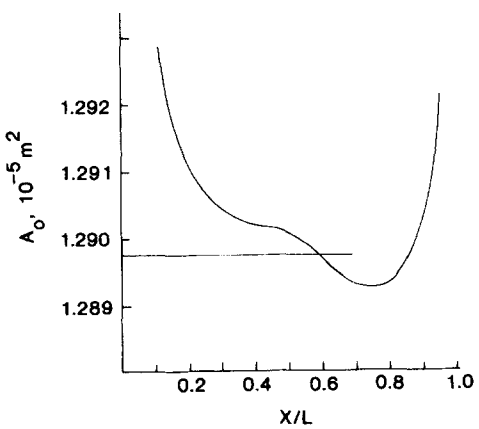

FIG. 10. Area at atmospheric pressure plotted as a function of the ratio of the position along the cylinder divided by its length. The value of A_0 obtained from the pressure calibration is also plotted as the straight horizontal line. The two curves intersect at $X/L = 0.585$.

TABLE II. Elastic distortion coefficient for steel piston and cylinder.

Method	21-MPa range b
Piston gauge intercomparison	4.21×10^{-12}/Pa
Elastic theory ($P_a = 0.5P_s$)	3.19×10^{-12}/Pa
Elastic theory, measured profile ($P_a = 0.842P_s$)	4.34×10^{-12}/Pa
Elastic theory, Bass model profile ($P_a = 0.828P_s$)	4.29×10^{-12}/Pa
Similarity method	4.06×10^{-12}/Pa

profile from the dimensional measurements using Eq. (3). (2) Determine the values of P_a/P_s and X/L where the downward break in the pressure profile curve occurs. (3) Calculate A_0 as the mean of the piston and cylinder areas using the radii for each at the X/L value where the downward break in the slope occurs. (4) Provided Eq. (2) is appropriate for the piston gauge design, calculate b using Eq. (2) and the value of P_a/P_s where the downward break in the slope occurs. (5) Calculate the effective area using Eq. (1).

D. Viscosity

After completing the pressure profile measurements using fluid 34, the system was carefully purged and the more viscous fluid 38 was installed. The pressure profile measurements were repeated and the results from the four nominal system pressures were compared with those obtained using the previous fluid.

The results for the two fluids were nearly identical. The profile curves, representing the four nominal system pressures, were averaged and plotted for each fluid in Fig. 11.

The viscosity of both fluids changes nearly linearly by a factor of 2 over this pressure range. The Bass model treats viscosity as a constant. The success of the Bass model in describing $P_a(X/L)/P_s$ is an indication that the role of viscosity in the operation of piston gauges is not yet understood.

IV. TEMPERATURE MEASUREMENTS

There are three sources of heat due to the operation of a piston gauge: (a) adiabatic heating in the fluid due to a rapid pressure change, (b) heat generated by friction in the fluid due to the flow up the annulus, and (c) heat generated by the rotation of the piston. Normally, the operating temperature of piston gauges is determined either on the base supporting the cylinder or on the lower end of the cylinder. The test ports in the gauge used in this study provided the opportunity to gain additional information on the effects due to all three sources of heat in the annulus. Differential temperature measurements between the fluid at the lower end of the piston, hereafter referred to as the "system", and various ports provided the temperature profile along the piston. Additional differential temperature measurements between the system and a thermally massive metal block at room temperature were also recorded.

A. Adiabatic effects

The piston gauge was not completely thermally isolated. Adiabatic conditions were only approximated in that the times involved in pressure changes are fractions of a second while times characteristic of heat flow are on the order of minutes. Adiabatic heating along the piston in the modified gauge is also greater than would be the case in a normal gauge due to the compression of the additional fluid in the test port.

Figue 12 shows an example of the adiabatic response. With the piston not rotating, the system was quickly pressurized to 14 MPa. The abrupt spike appearing in both the differential and system trace is the thermocouple response to the increase of temperature in the fluid due to adiabatic heating. In the differential trace, the spike quickly disappears due to heat flow into the surrounding steel from the very small

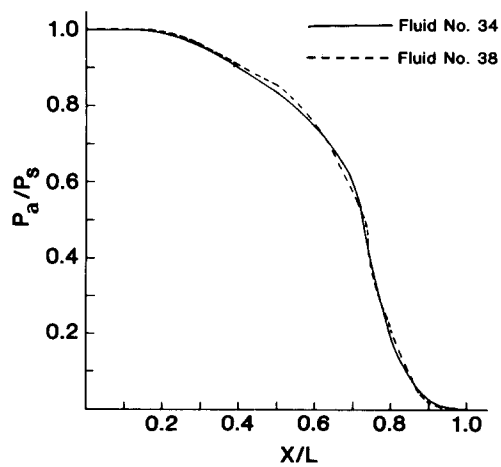

FIG. 11. Ratio of the pressure in the annulus between piston and cylinder to the pressure in the system for both fluid 34 and fluid 38 as a function of the ratio of the position along the cylinder to its length. The curves are the average for all four pressures for each fluid. Discrete data points have been omitted for clarity.

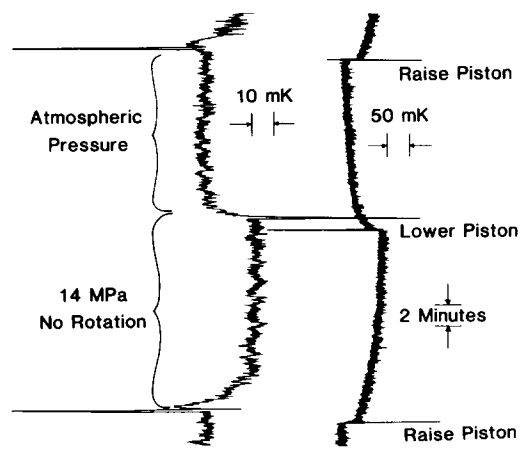

FIG. 12. Strip chart recorder trace of the temperature responses in the fluid to changes of pressure with the piston not rotating. The spikes are due to adiabatic heating. The left trace is the differential temperature between the selected port on the cylinder and the system. The right trace is the temperature of the system.

fluid volume. The slow rise in temperature that follows under the piston is many times that in the annulus and is the source of the heat causing the temperature increase in the system trace that requires several minutes to stabilize. Table III gives an indication of the temperature increases in the system due to adiabatic heating for both fluids.

B. Flow effects

The temperature changes due to the flow of the fluid up the annulus past the piston were also determined with the piston in a static position. With a thermocouple junction installed in the selected port, the piston was removed from the cylinder and the fluid was raised to the top of the cylinder. The gauge was then covered and allowed to come to thermal equilibrium usually requiring about 20 min. Next, the piston was installed taking care to assure no air was trapped under it, loaded with the appropriate weights, and adjusted to the proper reference level using the hand generator. Readings of the differential temperatures were taken when a constant rate of change existed between the temperature in the annulus and that of the system. System temperatures at the beginning of each run were initially equal to the nominal room temperature. This procedure was performed with the stationary piston positioned at 0°, 90°, 180°, 270°, and repeated at 0° relative to its original orientation in order to account for any change or irregularity in dimensions of the annulus. Temperature measurements at atmospheric pressure were made before and after each measurement at high pressure. The results of these measurements of fluid 34 are plotted in Fig. 13 as a function of normalized cylinder working length. Each point on the plot is the difference between the average of the five readings at pressure and the average of the six atmospheric pressure readings with a maximum standard deviation of about 2 mK.

The results of these measurements for fluid 38 are plotted in Fig. 14. For this case, the curves for 2.3 and 7 MPa are very similar to those obtained when using fluid 34 while the 14 and 21 MPa curves have significantly smaller slopes than the curves for the same pressure using fluid 34. The evidence suggests that at higher pressure the increased viscosity reduced the flow resulting in reduced temperatures.

A rough estimate for the differential temperature between the system and a point along the annulus due to flow alone can be determined using the following empirical equation:

TABLE III. Adiabatic heating system.

	Fluid 34		Fluid 38	
Pressure (MPa)	Initial thermocouple response (mK)	Net temperature increase (mK)	Initial thermocouple response (mK)	Net temperature increase (mK)
2.3	101	≃2	88	≃2
7	191	19	153	12
14	246	38	205	34
21	281	54	235	54

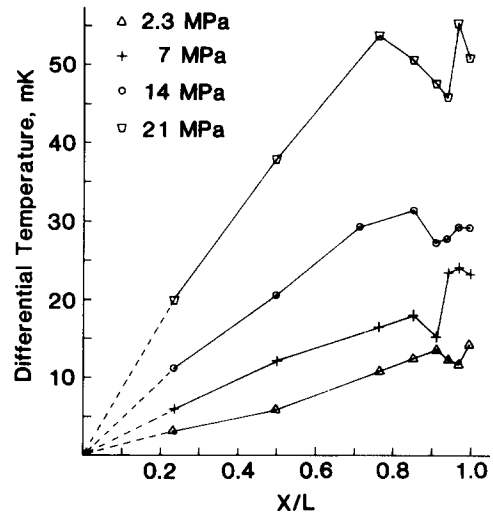

FIG. 13. Differential temperature between the fluid in the annulus and that in the system measured at four pressures for fluid 34. The curves are intended only as a guide to the eye.

$$\Delta T = \frac{(X/L)P}{\mu_0 + 0.16}, \tag{4}$$

where ΔT is in mK, P is the pressure in MPa, and μ_0 is the viscosity in P at room temperature and atmospheric pressure.

All of the curves of Figs. 13 and 14 have a segment that is nearly linear followed by a decrease and then an increase in temperature near the top end of the cylinder. The temperature patterns and the fact that diverging flow tends to be unstable suggest the presence of turbulence; however, the transition from laminar to turbulent flow occurs when the Reynolds number exceeds a critical value. According to Hanks[8] the critical Reynolds number for this apparatus is 2285. Since the Reynolds number describing the flow in the gauge is on the order of 0.01, it appears unlikely that the piston gauge experiences turbulent flow.

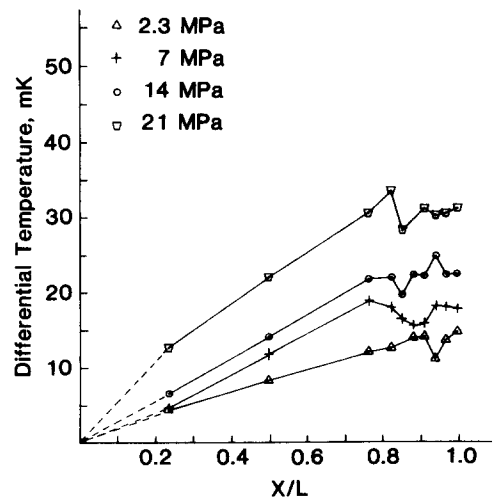

FIG. 14. Differential temperature between the fluid in the annulus and that in the system measured at four pressures for fluid 38. The curves are intended only as a guide to the eye.

The probable cause of the decrease in temperature is cooling of the fluid due to decompression. Since all of these temperature measurements were made after the temperature had become stable, there would be enough time for the flow to establish in the piston and cylinder the same temperature gradient observed in the fluid. Once the decompression had occurred, the fluid was reheated via the temperature gradient in the piston and cylinder.

C. Rotational effects

When the piston is rotated, heat is generated uniformly along the entire cylinder working length which increases the system temperature but does not change the differential temperature between the system and a point in the annulus, as was verified in several measurements. With rotation, the system temperature increases at about twice the rate as is the case without rotation.

The average thermal expansion for a steel piston and cylinder assembly is on the order of 20 ppm per °C. The precision of pressure measurement of such an assembly could be on the order of 5 ppm. If it is assumed, for the sake of establishing a figure of merit, that the total uncertainty due to temperature effects must not exceed the precision, then an uncertainty in the temperature measurements of 250 mK is tolerable for this case. After a piston gauge is allowed to operate for several minutes differences due to adiabatic heating have come to equilibrium, the only cause of temperature difference between the low end of the cylinder and some location along the annulus is that due to the flow of the pressurizing fluid. The temperature difference is a function of pressure, viscosity, and location along the engagement length. For the piston cylinder assembly, fluids, and pressures employed in this study, the maximum temperature difference measured over the entire engagement length was less than 60 mK, suggesting that the uncertainty resulting from temperature measurements at the lower end of the cylinder does not exceed the figure of merit.

In general, temperature measurements of the piston and cylinder assembly should be made on the outer surface of the cylinder at the level where the break in the slope of the pressure profile curve occurs. For the sake of convenience, however, temperature measurements are usually made at a place far removed from that site. The effect of the compromise in location must be considered on a case-by-case basis because of the wide variety in gauge design and choice of materials of construction.

ACKNOWLEDGMENTS

The authors would like to acknowledge the assistance given by members of the NBS staff, including J. H. Colwell, G. W. Burns, W. Markus, C. R. Tilford, F. G. Long, and J. C. Houck of the Temperature and Pressure Measurements and Standards Division, R. C. Veale of the Length and Mass Measurements and Standards Division; R. W. Davis of the Fluid Engineering Division; and R. E. Lack of the Instrument Shops Division. Also, they greatly appreciate the cooperation and equipment provided by members of the piston gauge manufacturing community.

[1]P. L. M. Heydemann and B. E. Welch, *Experimental Thermodynamics. Volume II: Experimental Thermodynamics of Non-reacting Fluids*, edited by B. Le Neindre and B. Vodar (Butterworths, London, 1975), pp. 147–202.
[2]S. Lewis and G. N. Peggs, *The Pressure Balance: A Practical Guide to Its Use* (National Physical Laboratory, Teddington, England, 1979).
[3]J. L. Cross, *Reduction of Data for Piston Gage Pressure Measurements*, NBS Monograph 65 (National Bureau of Standards, Washington, D. C., 1963).
[4]A. H. Bass, J. Phys. E. **11**, 682 (1978).
[5]D. P. Johnson and D. H. Newhall, Trans. ASME **75**, 301 (1953).
[6]R. S. Dadson, R. G. P. Greig, and A. Horner, Metrologia **1**, 55 (1964).
[7]M. K. Zhokhovskii, *Theory and Design of Instruments with Packing-Free Pistons* (Moscow, 1959).
[8]R. W. Hanks, AIChE J. **26**, 152 (1980).